

## RESEARCH ARTICLE

# Modeling stochastic phenotype switching and bet-hedging in bacteria: stochastic nonlinear dynamics and critical state identification

Chen Jia<sup>1,2</sup>, Minping Qian<sup>1</sup>, Yu Kang<sup>3</sup> and Daquan Jiang<sup>1,4,\*</sup>

<sup>1</sup> LMAM, School of Mathematical Sciences, Peking University, Beijing 100871, China

<sup>2</sup> Beijing International Center for Mathematical Research, Beijing 100871, China

<sup>3</sup> CAS Key Laboratory of Genome Sciences and Information, Beijing Institute of Genomics, Chinese Academy of Sciences, Beijing 100101, China

<sup>4</sup> Center for Statistical Science, Peking University, Beijing 100871, China

\* Correspondence: jiangdq@math.pku.edu.cn

Received September 7, 2014; Revised November 5, 2014; Accepted November 14, 2014

Fluctuating environments pose tremendous challenges to bacterial populations. It is observed in numerous bacterial species that individual cells can stochastically switch among multiple phenotypes for the population to survive in rapidly changing environments. This kind of phenotypic heterogeneity with stochastic phenotype switching is generally understood to be an adaptive bet-hedging strategy. Mathematical models are essential to gain a deeper insight into the principle behind bet-hedging and the pattern behind experimental data. Traditional deterministic models cannot provide a correct description of stochastic phenotype switching and bet-hedging, and traditional Markov chain models at the cellular level fail to explain their underlying molecular mechanisms. In this paper, we propose a nonlinear stochastic model of multistable bacterial systems at the molecular level. It turns out that our model not only provides a clear description of stochastic phenotype switching and bet-hedging within isogenic bacterial populations, but also provides a deeper insight into the analysis of multidimensional experimental data. Moreover, we use some deep mathematical theories to show that our stochastic model and traditional Markov chain models are essentially consistent and reflect the dynamic behavior of the bacterial system at two different time scales. In addition, we provide a quantitative characterization of the critical state of multistable bacterial systems and develop an effective data-driven method to identify the critical state without resorting to specific mathematical models.

**Keywords:** phenotypic heterogeneity; phenotypic variation; multistability; gene network; stochastic gene expression

## INTRODUCTION

Bacteria in the wild exist in ever-changing environments and have to surmount the challenges posed by environmental fluctuations. Numerous experiments have confirmed that multiple distinct phenotypes can coexist within an isogenic bacterial population [1–10]. This phenotypic heterogeneity in genetically identical cells has received increasing attention in recent years since it could help the bacteria to survive in rapidly changing environments [11,12]. In the framework of traditional population genetics, a bacterial population enhances its fitness via

genetic changes caused by mutation or recombination. However, extracellular conditions can change so rapidly that adaptation only by mutation or recombination would be too slow. One solution to this problem is to allow individual cells to stochastically switch among multiple phenotypes without genetic changes, a phenomenon widely known as stochastic phenotype switching [13–18]. Generally, the multiple phenotypes within an isogenic bacterial population result from the multiple steady-state expression levels of a group of stress-related genes. Such kind of gene expression pattern with multiple steady-state expression levels are widely known as multistability [3,7].

Phenotypic heterogeneity is a widespread phenomenon in the bacterial realm. Examples of phenotypic heterogeneity include lactose utilization in *Escherichia coli* [19], competence development in *Bacillus subtilis* [20–22], sporulation in *Bacillus subtilis* [23–26], and persistence in *Mycobacterium tuberculosis* [27–29]. The potential function of phenotypic heterogeneity with stochastic phenotype switching is generally understood to be a bet-hedging strategy [7,12,30,31], a term originating from finance. In response to fluctuating environments, a heterogeneous bacterial population could optimize its fitness by altering the proportion of cells in each subpopulation via stochastic phenotype switching to achieve an optimal ‘investment portfolio’.

To study the evolution of heterogeneous bacterial populations, a number of Markov chain models have been proposed at the cellular level [1,6,14,16,17,32–34]. These models assumed *a priori* that the bacterial population has multiple distinct phenotypes. In these chain models, each phenotype is modeled as a state of the Markov Chain and stochastic phenotypic switching is modeled as the state transition of the Markov chain. However, these models take phenotypic heterogeneity and stochastic phenotypic switching for granted and fail to account for their underlying molecular mechanisms.

Recent research has demonstrated that phenotypic heterogeneity within isogenic bacterial populations often results from the feedback circuitry of the gene regulatory network [35,36]. To account for the molecular mechanism of phenotypic heterogeneity, a number of deterministic models have been proposed at the molecular level [19,22,27,29,37]. In these models, different steady states of gene expression are described as different stable fixed points (attractors) of a deterministic system composed of several ordinary differential equations which are written down based on the regulatory relationship of the gene network. However, deterministic models cannot provide a correct description of many important experimental phenomena, such as stochastic phenotype switching and bet-hedging. In every deterministic model, if the expression level of an individual cell lies in an attraction basin at a particular time, it will never leave this attraction basin and thus phenotype switching will never occur.

Although deterministic models can give rise to multiple attractors and attraction basins, they do not allow transitions among different attraction basins. One solution to this problem is to consider stochastic effects, which allow the system to transition among different attraction basins and thus drive stochastic phenotype switching. This fact is analogous to the simulated annealing techniques in optimization problems, in which noise is indispensable to make the search escape from the trap of local minimum points and reach the global minimum point. To better understand the role that stochastic effects

play in bistable systems, Qian and coworkers studied the relations between deterministic and stochastic nonlinear dynamics in great detail [38–43]. However, their models are usually so abstract and oversimplified that they cannot be directly applied to practical problems with experimental data and observations.

Stochastic effects are extremely important not simply because they are indispensable for the model to generate phenotype switching, but because gene expression is an inherently stochastic process. Recent developments of single-cell and single-molecule experiments have shown that many important cellular processes, such as transcription, translation, replication, and gene regulation, are inherently stochastic [44–53]. Due to stochastic effects, the expression levels of the stress-related genes in a multistable system will have a multimodal distribution.

In this paper, we propose a unified nonlinear stochastic model of multistable bacterial systems at the molecular level based on a core double-positive-feedback gene network. By studying its stochastic nonlinear dynamics, we show that our model not only provides a clear description of phenotypic heterogeneity, stochastic phenotype switching, and bet-hedging within isogenic bacterial populations, but also provides a deeper insight into the analysis of multidimensional experimental data, such as gene expression data and the data of more comprehensive indicators like the forward scatter (FSC) and the side scatter (SSC) measured by flow cytometry.

Next, we use the mathematical tool of large deviation theory established by Freidlin and Wentzell [54] to show that every multistable dynamical system under a small random perturbation can be approximated by a Markov chain with multiple states, each corresponding to an attraction basin of the multistable system. In this way, our stochastic model at the molecular level can be reduced to a Markov chain model at the cellular level. This justifies the wide applications of previous Markov chain models of population evolution, in particular, the Markov chain model proposed by Lander and coworkers [33] about the dynamics of the phenotypic proportions in human breast cancer cell lines.

In addition, we point out a widespread misunderstanding on the analysis of gene expression data, inspired by our recent work about antibiotic resistance in *Escherichia coli*. Previous studies tended to think that phenotypic heterogeneity can be identified by the multistable expression of a single pivotal gene (reviewed in Refs. [2,7]). However, phenotypic heterogeneity in bacterial populations often results from the interaction of a group of stress-related genes. We use simulation results to show that in many cases, the expression data of a group of genes give rise to an apparent multimodal distribution, however, we cannot observe the multistable expression if we only focus on the expression data of a single gene. This

suggests that the traditional method to identify phenotypic heterogeneity by measuring the expression of a single pivotal gene is sometimes ineffective.

Finally, we use our stochastic model to provide an answer to the important question of identifying the critical state of multistable bacterial systems. In our stochastic model, there is a saddle lying on the boundary of two adjacent attraction basins which characterizes a critical state between two steady states of gene expression. The critical state is not targeted in the previous work since it is rarely observed in experiments and cannot be estimated by simple statistical analysis of gene expression data. However, the identification of the critical state has drawn increasing attention in recent years since it is closely related to the early diagnosis of complex diseases [55,56]. In this paper, we develop an effective method to identify the critical state of multistable bacterial systems using the time-course data of gene expression without resorting to specific mathematical models.

## METHODS

The parameters used to draw the figures in the main text are chosen as  $\alpha = 1$ ,  $\beta = 2$ ,  $\gamma = 0.8$ ,  $K = 0.05$ ,  $\delta = 0$ , and  $n = 6$ . The inducer concentration  $a$  and the two noise levels,  $\varepsilon$  and  $\eta$ , are chosen appropriately when drawing different figures.

## RESULTS

### Model

In natural bacterial systems, phenotypic heterogeneity and stochastic phenotype switching always originate from the feedback circuitry of the regulatory network which governs a group of stress-related genes. To better understand the general principles behind phenotypic heterogeneity, we illustrate the gene regulatory networks that govern some best-understood multistable systems in bacteria (Figure 1A–D). A crucial similarity shared by these examples is that the wiring of the gene regulatory network forms a double-positive-feedback loop. To establish a unified model of these bacterial systems, we focus on the core double-positive-feedback gene network depicted in Figure 1E, where, protein X is the product of a pivotal stress-related gene, i.e., gene  $X$ , protein Y is a transcription factor which activates the expression of gene  $X$ , and A is an inducer whose concentration reflects the fluctuations in extracellular environmental conditions, such as fluctuations in temperature, pH, and concentrations of nutrients and toxins [23,27].

We use lowercase letters  $x$ ,  $y$ , and  $a$  to denote the concentrations of X, Y, and A, respectively. Since gene expression is an inherently stochastic process, the

dynamics of  $x$  and  $y$  can be described by the following two-dimensional system of stochastic differential equations (SDEs):

$$\begin{cases} \dot{x} = -\alpha(x - F(a, y)) + \sqrt{2\varepsilon}\xi_x, \\ \dot{y} = -\beta(y - G(x)) + \sqrt{2\eta}\xi_y, \end{cases} \quad (1)$$

where  $F(a, y)$  describes the activation of protein X by inducer A and protein Y,  $G(x)$  describes the activation of protein Y by protein X, and  $\alpha$  and  $\beta$  are two parameters characterizing the response speeds of proteins X and Y, respectively. In addition,  $\xi_x$  and  $\xi_y$  are two independent standard white noises satisfying  $\langle \xi_x(t) \rangle = \langle \xi_y(t) \rangle = 0$  and  $\langle \xi_x(t)\xi_x(t') \rangle = \langle \xi_y(t)\xi_y(t') \rangle = \delta(t-t')$ . Since the fluctuations in the levels of proteins X and Y can be different, we use two noise levels  $\varepsilon$  and  $\eta$  to describe their stochastic fluctuations. We emphasize here that noise in gene regulatory networks generally comes from a great number of sources and may not be subsumed into white noises. Fortunately, the specific noise distributions will hardly affect the main results of this paper. To make our discussion friendly to both theoretical and experimental biologists, we would like to use white noises to describe noise in gene expression. For the rationality of this assumption, please see Discussion.

If we ignore stochastic effects, then the stochastic system (1) can be reduced to the following deterministic system as the two noise levels,  $\varepsilon$  and  $\eta$ , tend to zero:

$$\dot{x} = -\alpha(x - F(a, y)), \quad \dot{y} = -\beta(y - G(x)). \quad (2)$$

We note that the fixed points of this deterministic system are the solutions to the following equations:  $x - F(a, G(x)) = 0$  and  $y = G(x)$ . In natural bacterial systems, the most common expression of  $F(a, G(x))$  has the following form (see Supplementary Information):

$$F(a, G(x)) = \frac{\gamma x^n}{K + x^n} + (\mu a + \delta), \quad (3)$$

where the Hill function  $\gamma x^n / (K + x^n)$  with  $n > 1$  describes the activation of gene  $X$  by protein Y, the term  $\mu a$  describes the activation of protein X by inducer A, and the term  $\delta$  describes a basal expression level of gene  $X$  independent of the activation of protein Y.

It turns out that the deterministic system (2) has one or three fixed points under different inducer concentrations (Figure 2A). To be specific, the inducer concentration  $a$  has two threshold levels,  $a_0$  and  $a_1$ . If  $a < a_0$  or  $a > a_1$ , the system has only one fixed point (Figure 2A). If  $a < a_0$ , the only attractor  $(x_L, y_L)$  describes the phenotype of low-expressing cells in which gene  $X$  is inactivated. If  $a > a_1$ , the only attractor  $(x_H, y_H)$  describes the phenotype of high-expressing cells in which gene  $X$  is activated. If  $a_0 < a < a_1$ , however, the system has three fixed points,

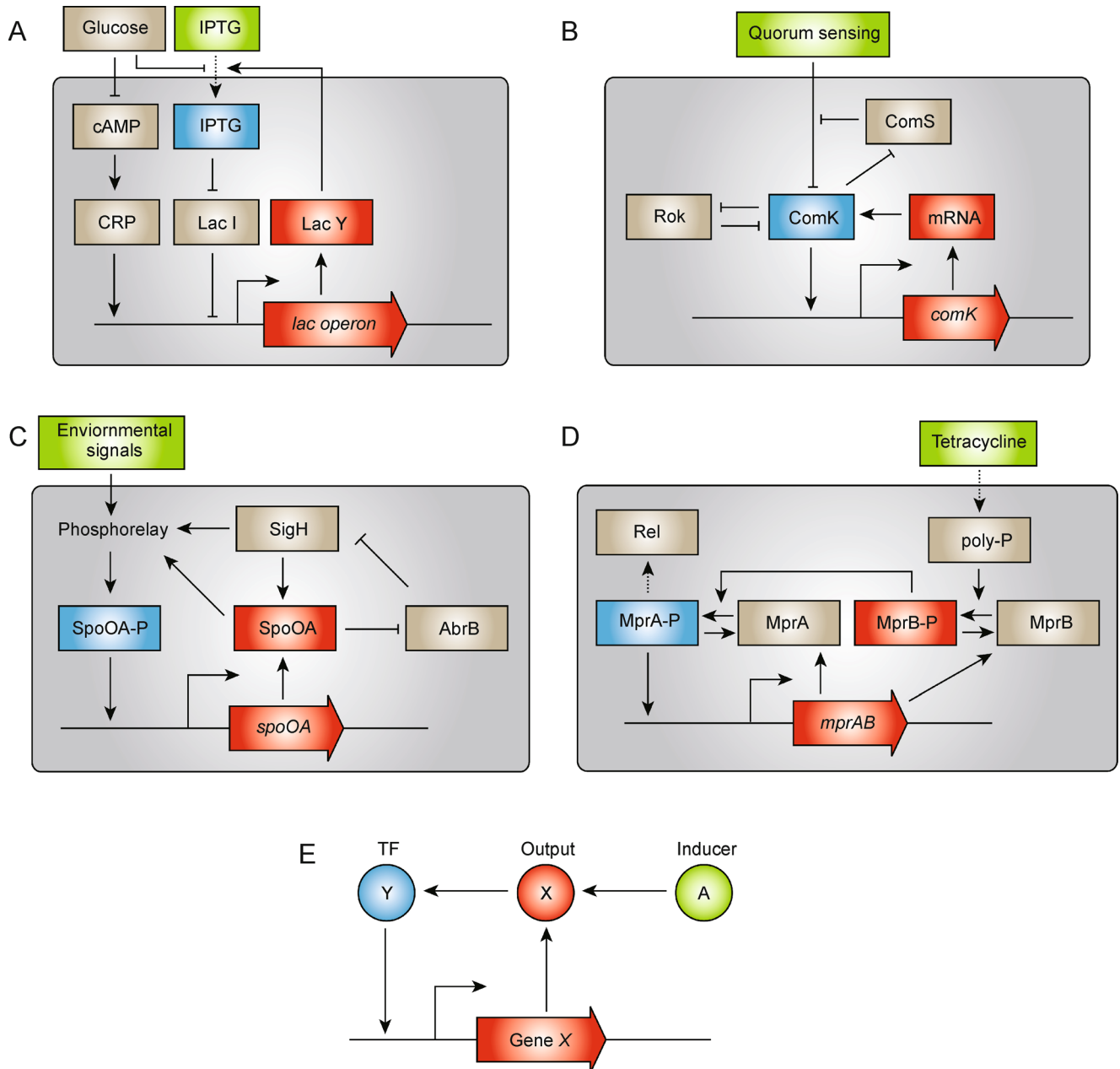


**Figure 1. Schematic models of bacterial systems with phenotypic heterogeneity.** (A–D) Examples of naturally occurring bacterial systems with phenotypic heterogeneity. (A) Lactose utilization in *E. coli* [19]. (B) Competence development in *B. subtilis* [20]. (C) Sporulation in *B. subtilis* [23]. (D) Persistence in *M. tuberculosis* [29]. (E) The core double-positive-feedback gene network shared by A–D. X (red) is the product (protein or mRNA) of a pivotal stress-related gene. Y (blue) is a transcription factor which activates the expression of gene X. A (green) is an inducer whose concentration reflects extracellular environmental conditions.

including two attractors,  $(x_L, y_L)$  and  $(x_H, y_H)$ , and a saddle  $(x_M, y_M)$  (Figure 2A, B), where the two attractors describe the phenotypes of low- and high-expressing cells, respectively, whereas the saddle is a critical state between the two steady states of gene expression. Mathematically, each attractor of a deterministic system has an attraction basin, and two adjacent attraction basins are separated by a boundary (Figure 2B).

### Phenotypic heterogeneity and bet-hedging

In the recent decade, single-cell and single-molecule experiments have made significant progresses and shown that gene expression is an inherently stochastic process. Although deterministic models, such as the deterministic system (2), can give rise to multiple attractors and attraction basins, they cannot provide a correct descrip-

tion of stochastic phenotype switching and bet-hedging. These two facts show that the reduction from the stochastic system (1) to the deterministic system (2) is inappropriate.

In the following discussion, we focus on the stochastic system (1) in which the two noise levels,  $\varepsilon$  and  $\eta$ , are strictly positive. Although the system does not satisfy detailed balance, we can still obtain an approximate steady-state probability distribution  $p_s(a, x, y)$  of the system (see Supplementary Information), which has the following form:

$$p_s(a, x, y) = \frac{1}{Z} \exp \left\{ -\frac{1}{\varepsilon} U(a, x, y) \right\}, \quad (4)$$

where  $Z$  is a normalization constant and  $U(a, x, y)$  is an approximate global potential, also called landscape, of the system defined as

$$U(a, x, y) = \frac{\varepsilon\beta}{2\eta} (y - G(x))^2 + \alpha \int_0^x (u - F(a, G(u))) du. \quad (5)$$

We make a crucial observation that the fixed points of the deterministic system (2) are exactly the solutions to the equation  $\partial_x U(a, x, y) = \partial_y U(a, x, y) = 0$ . This shows that the attractors of the deterministic system are the local minimum points of the approximate global potential  $U(a, x, y)$  and thus are the local maximum points of the steady-state distribution  $p_s(a, x, y)$ . From Figure 2C–E, we see that the steady-state distribution of the levels of proteins X and Y is controlled by the inducer concentration  $a$ . If  $a < a_0$ , the steady-state distribution has only the left peak, suggesting that the bacterial population contains almost exclusively low-expressing cells under favorable conditions (Figure 2C). If  $a_0 < a < a_1$ , the steady-state distribution has both the left and right peaks, each corresponding to a phenotype. With the increase of the inducer concentration, a larger fraction of cells will switch from the low- to the high-expressing subpopulation to maximize survival (Figure 2D). If  $a > a_1$ , the left peak of the steady-state distribution disappears, suggesting that the bacterial population contains almost exclusively high-expressing cells under unfavorable conditions (Figure 2E). The above discussion clearly explains how the bet-hedging strategy could help the bacterial population better adapt to rapidly changing environmental conditions.

Generally, the steady-state gene expression levels in a multistable bacterial system have a multimodal distribution, which can be viewed as the superposition of multiple monomodal distributions, each concentrated within an attraction basin. The attractors are the locally most-probable states and thus are most likely to be observed in experiments. Based on the stochastic system (1), we simulate the time course of the levels of proteins X and Y

in a single cell (Figure 2B). The simulation result shows that the gene expression data are generally distributed around the attractors and are rarely distributed around the boundary of the attraction basins. These facts clearly show that each phenotype of a bacterial population cannot be simply described as an attractor of the deterministic model, but should be understood as a monomodal distribution concentrated within an attraction basin.

### A widespread misunderstanding on the analysis of gene expression data

Phenotypic heterogeneity in isogenic bacterial populations often results from the interaction of a group of stress-related genes and biochemical species. Previous studies tended to think that phenotypic heterogeneity can be identified by the multistable expression of a single pivotal gene (reviewed in Refs. [2,7]). In experiments, however, it often happens that the steady-state expression data of a single gene does not display a multimodal distribution, and only when a subpopulation of cells are sorted out to start from some extreme initial conditions, the multimodal distribution can be observed at certain times before reaching the steady state. Thus it is rather difficult to determine whether the bacterial population has multiple phenotypes or not. To explain these experimental phenomena, we point out that phenotypic heterogeneity often results from the interaction of a group of stress-related genes and may not be observed if we only focus on the expression data of a single gene. In our recent study about antibiotic resistance in *Escherichia coli* (unpublished work), we found that the expression data of the hydrolase gene only lead to a monomodal distribution, whereas the expression data of a group of stress-related genes lead to an apparent multimodal distribution.

We now use our stochastic model to account for this interesting phenomenon. Based on the stochastic system (1), we simulate the steady-state levels of proteins X and Y in 500,000 virtual cells under a set of model parameters (Figure 2F). From the simulation result, we see that the two-dimensional gene expression data are distributed around two attractors in the phase plane and lead to a bimodal distribution, which can be viewed as the superposition of two monomodal distributions. Although these two monomodal distributions are concentrated within two different attraction basins in the phase plane, there is an obvious overlap between their marginal distributions, whose superposition, which represents the steady-state distribution of the level of protein Y, has only one peak (Figure 2G). This suggests that the traditional idea to identify phenotypic heterogeneity by the multistable expression of a single pivotal gene is sometimes ineffective. The above discussion also shows that our stochastic model can help us gain a deeper insight into the

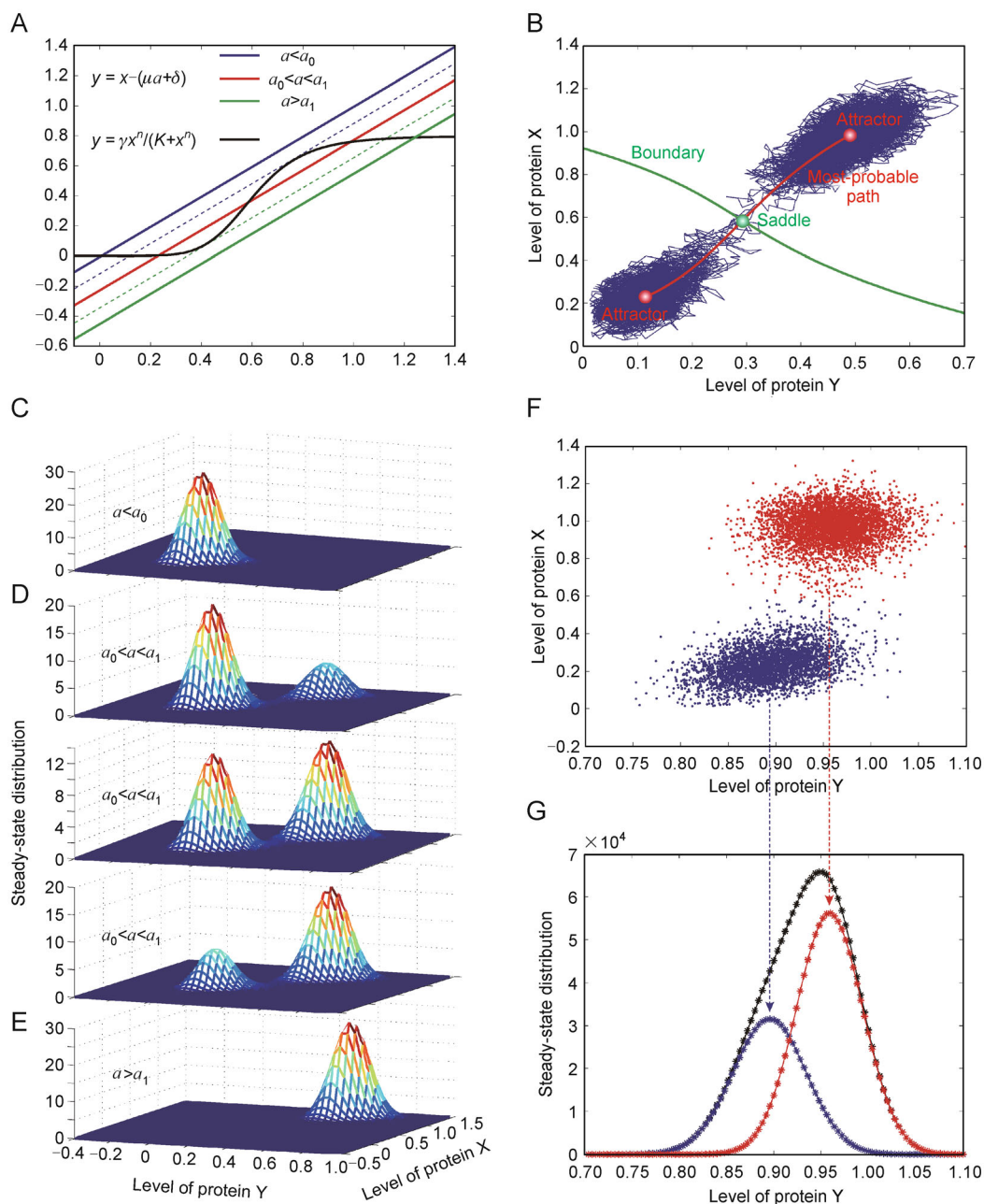


**Figure 2. Stochastic description of multistability.** (A) Numbers of fixed points under different inducer concentrations. The curve represents the Hill function  $y = \gamma x^n / (K + x^n)$  and the lines represent the function  $y = x - (\mu a + \delta)$ . The intersections of the curve and the line give the positions of the fixed points. (B) The simulation data of the time course of the levels of proteins X and Y in a single cell. When  $a_0 < a < a_1$ , the deterministic model has three fixed points, including two attractors and a saddle, which lies on the boundary of two attraction basins. The expression levels of the cell stay around the two attractors at most times and cross the boundary around the saddle. (C–E) The steady-state probability distribution of the levels of proteins X and Y. (C) When  $a < a_0$ , the steady-state gene expression levels have a monomodal distribution, which attains its unique maximum at the attractor  $(x_L, y_L)$ . (D) When  $a_0 < a < a_1$ , the steady-state gene expression levels have a bimodal distribution, which attains two maxima at both the two attractors,  $(x_L, y_L)$  and  $(x_H, y_H)$ . (E) When  $a > a_1$ , the steady-state gene expression levels have a monomodal distribution, which attains its unique maximum at the attractor  $(x_H, y_H)$ . (F) The simulation data of the steady-state levels of proteins X and Y in 500,000 virtual cells under a set of model parameters. The two-dimensional gene expression data are distributed around two attractors and thus lead to an apparent bimodal distribution. (G) The marginal distribution of the level of protein Y based on the two-dimensional gene expression data. The blue and red curves represent the marginal distributions of low- and high-expressing cells, respectively, and the black curve represents the marginal distribution of all cells. There is an obvious overlap between the marginal distributions of low- and high-expressing cells, resulting in a monomodal overall marginal distribution.

pattern behind multidimensional experimental data.

### From the molecular level to the cellular level

We have seen that our stochastic model provides a clear description of phenotypic heterogeneity and bet-hedging within isogenic bacterial populations at the molecular level. However, more widely used models in the previous work are Markov chain models at the cellular level. These models assume *a priori* that the bacterial population has multiple distinct phenotypes, each of which corresponds to a state of the Markov chain and can switch to other phenotypes with certain transition rates. This raises the question of whether the two kinds of models, our stochastic model at the molecular level and the Markov chain models at the cellular level, are consistent in some way or not. We now use the mathematical tool of large deviation theory established by Freidlin and Wentzell [54] to answer this question.

The Freidlin-Wentzell theory is mainly concerned about the dynamic behavior of a multistable dynamical system under random perturbations, such as the stochastic system (1), when the noise level is not too large. The conclusions of the Freidlin-Wentzell theory are not very intuitive at first sight and the proofs of them are rather tedious. Readers who are interested in the mathematical aspects of the Freidlin-Wentzell theory may refer to [54,57]. To make readers understand this useful mathematical tool, we would like to list the major results of the Freidlin-Wentzell theory as follows.

**Basic Result 1.** No matter how small the noise level is, the accumulation of the stochastic forces will make the system escape from the trap of an attraction basin and enter another attraction basin. Before the system escapes from an attraction basin, it will spend most of the time staying around the attractor and spend little time staying around the boundary of the attraction basin. These facts can be seen from our numerical simulation in Figure 2B and Figure 3A.

**Basic Result 2.** Each point  $x$  in an attraction basin has a local potential  $V(x)$  called the quasi-potential. If the system has a global potential  $U(x)$ , as in Equation (5), then the quasi-potential  $V(x)$  can be calculated explicitly as

$$V(x) = 2(U(x) - U(x_0)), \quad (6)$$

where  $x_0$  is the attractor in this attraction basin. When the system escapes from one attraction basin to another, it must cross the boundary around a specific point  $y_0$  where the quasi-potential attains its minimum. In most cases, the minimum point  $y_0$  of the quasi-potential on the boundary is exactly the saddle of the system. These facts can be seen from our numerical simulation in Figure 2B.

**Basic Result 3.** The time needed for the system to escape

from an attraction basin is referred to as the escape time. The escape time  $T$  from an attraction basin approximately follows an exponential distribution. The mean escape time  $\langle T \rangle$ , which is approximately the time constant of the exponential distribution, has the form of

$$\langle T \rangle \doteq k \exp\left(\frac{1}{2\varepsilon}V_0\right), \quad (7)$$

where  $k$  is a positive constant,  $\varepsilon$  is the noise level, and  $V_0 = V(y_0)$  is the minimum value of the quasi-potential on the boundary. By Basic Result 2, if the system has a global potential  $U(x)$ , then  $V_0/2 = U(y_0) - U(x_0)$ , which represents the potential difference between the minimum point  $y_0$  of the potential on the boundary and the attractor  $x_0$ . These facts can be seen from our mathematical derivations in Supplementary Information.

It is a well-known result that the time needed for a Markov chain to make a state transition follows the exponential distribution. The Freidlin-Wentzell theory tells us that the escape time from each attraction basin approximately follows an exponential distribution. This shows that if we combine each attraction basin into a state, then the stochastic system with multiple attractors can be approximated by a Markov chain with multiple states at the time scale of  $\exp(1/\varepsilon)$ . When the noise level  $\varepsilon$  is small,  $\exp(1/\varepsilon)$  becomes very large. This shows that the approximate Markov chain reflects the long-term dynamic behavior of the stochastic system.

According to the above discussion, each stochastic model of a multistable system at the molecular level can be reduced to a Markov chain model at the cellular level. These two kinds of models at two different levels are essentially consistent and reflect the dynamic behavior of the system at two different time scales. For instance, the stochastic model (1) proposed in this paper has two attraction basins when  $a_0 < a < a_1$ , and thus can be approximated by a Markov chain model with two states, each corresponding to a phenotype. If the feedback architecture of the gene network becomes more complicated, then the stochastic system may possess three or more attraction basins and thus can be approximated by a Markov chain model with three or more states. For examples of Markov chain models with two, three, or four states, readers may refer to Refs. [16,17,33].

### Stochastic phenotype switching

To survive in rapidly changing environments, a heterogeneous bacterial population may allow individual cells to stochastically switch among multiple phenotypes, ensuring that some cells are always prepared for an unforeseen environmental fluctuation. This kind of phenotype switching is stochastic and temporary: An individual cell may switch to an alternative state at a random time

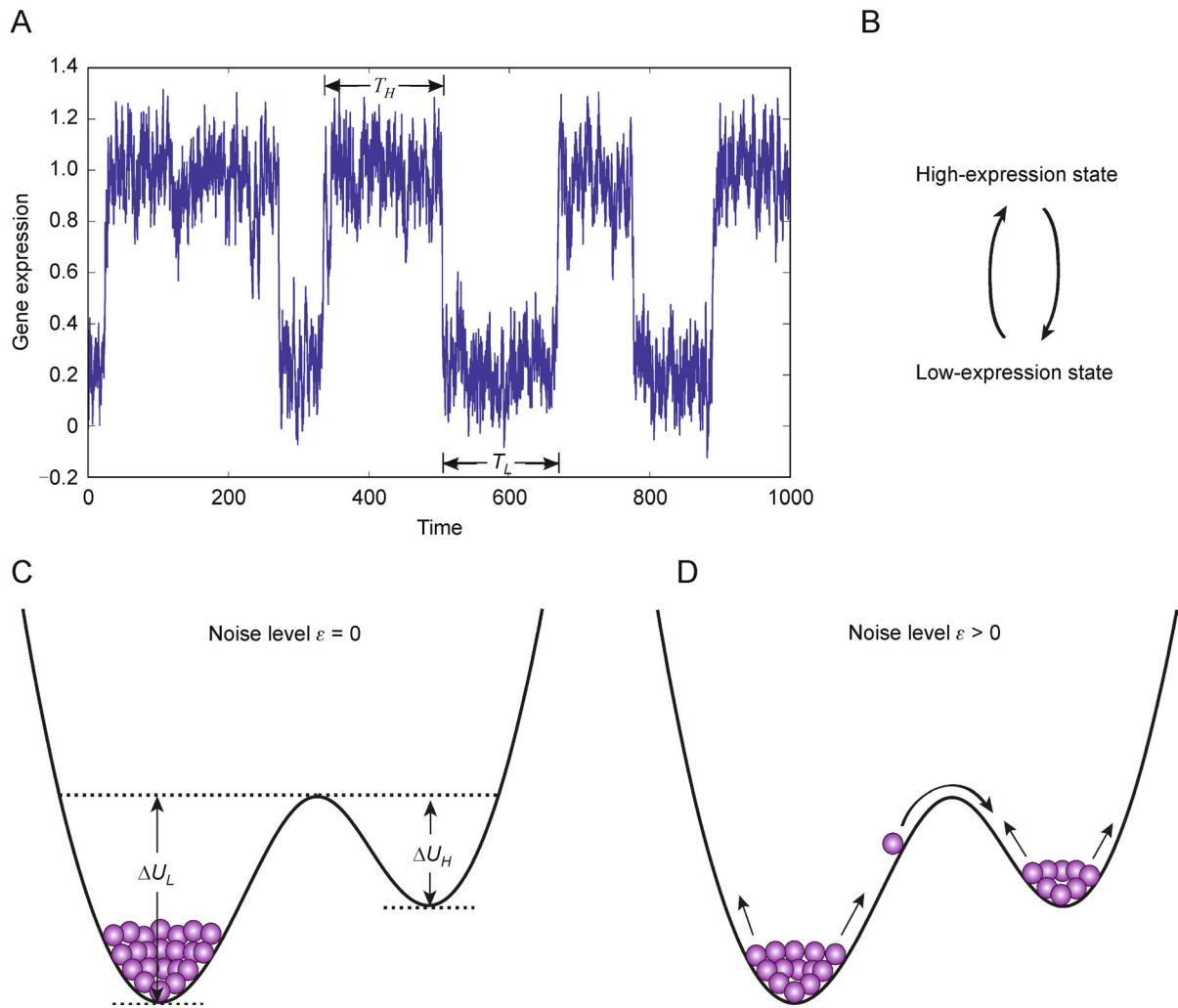


**Figure 3. Stochastic phenotype switching driven by stochastic forces.** (A) The simulation data of the time course of the level of protein X in a single cell. The cell switches between the low- and high-expression states at certain random times. (B) The simplified dynamics of the stochastic system (1) as a two-state Markov chain. (C) The steady-state behavior of the system when the noise level  $\varepsilon$  is zero. The curve represents the one-dimensional effective potential  $U(a, x, G(x))$ . If the low-expressing cells are sorted out at a particular time, then all cells will stay in the low-expression state forever and phenotype switching is impossible. (D) The steady-state behavior of the system when the noise level  $\varepsilon$  is positive. The accumulation of stochastic forces will drive individual cells to surmount the potential barrier and make a state transition.

and switch back again after some random time. Even without a significant change in environmental conditions, stochastic phenotype switching still exists. Stochastic phenotype switching has been observed in a wide range of bacterial species. As an example, upon encountering nutrient limitation, a minority of *Bacillus subtilis* cells transiently enter the competent state with the capability for DNA uptake from the environment before returning to vegetative growth [20].

To better understand the principle behind stochastic phenotype switching, we simulate the time course of the level of protein X in an individual cell based on the stochastic system (1) (Figure 3A). The simulation result

shows that the cell switches between the low- and high-expression states at certain random times. The Freidlin-Wentzell theory shows that the escape times  $T_L$  and  $T_H$  from the low- and high-expression states approximately follow exponential distributions. The mean escape times,  $\langle T_L \rangle$  and  $\langle T_H \rangle$ , have the following form (see Supplementary Information and Basic Result 3):

$$\begin{aligned} \langle T_L \rangle &\doteq \frac{2\pi}{\sqrt{\kappa_L \kappa_M}} \exp\left(\frac{1}{\varepsilon} \Delta U_L\right), \\ \langle T_H \rangle &\doteq \frac{2\pi}{\sqrt{\kappa_H \kappa_M}} \exp\left(\frac{1}{\varepsilon} \Delta U_H\right), \end{aligned} \quad (8)$$

where  $\Delta U_L$  and  $\Delta U_H$  are the potential differences between the saddle and the two attractors (Figure 3C) and  $\kappa_L$ ,  $\kappa_M$ , and  $\kappa_H$  are the curvatures of the one-dimensional effective potential  $U(a, x, G(x))$  at  $x_L$ ,  $x_M$ , and  $x_H$ , respectively. At the time scale of  $\exp(1/\varepsilon)$ , the dynamic behavior of the stochastic system (1) can be approximated by a Markov chain model with two states (Figure 3B).

According to Equation (8), the mean escape time is an exponential function of the potential barrier. The higher the potential barrier, the longer time is needed for a cell to make a state transition. Equation (8) also shows that the mean escape times have the time scale of  $\exp(1/\varepsilon)$ . This suggests that stochastic phenotype switching is a long-term dynamic behavior of the system. When the noise level  $\varepsilon$  is small, the escape time may be longer than the time of cell division. For a fraction of cells, stochastic phenotype switching may not occur in a single cell cycle, and thus they can pass their phenotypic state to the next generation.

If there were no stochastic effects, the phenotype of each individual cell would never change. Specifically, if the low-expressing cells are sorted out at a particular time, then all cells will stay in the low-expression state forever and phenotype switching is impossible (Figure 3C). In the presence of stochastic effects, however, the accumulation of stochastic forces will drive individual cells to surmount the potential barrier and make a state transition (Figure 3D). This suggests that stochasticity in gene expression is the driving force for stochastic phenotype switching.

### Importance of the critical state

We have seen that at certain ranges of the inducer concentration, the two attractors of the stochastic system (1) are separated by a boundary, forming two attraction basins. The saddle of the system lies exactly on the boundary of the two attraction basins (Figure 2B) and thus characterizes a critical state between the two steady states of gene expression. This saddle is not targeted in the previous work since it is rarely observed in experiments and cannot be estimated by simple statistical analysis of gene expression data. However, the identification of the critical state has drawn increasing attention in recent years due to the following three reasons.

First, the saddle represents a critical level of gene expression. Recent studies on complex diseases show that any disease progression can be divided into a normal state, a pre-disease state, and a disease state [55,56], similar to the low-expression state, the critical state, and the high-expression state described in this paper. Once the expression levels of the disease-related genes in a person is close to the saddle, we have good reasons to believe that this person is in a pre-disease state and is at high risk of disease progression. This suggests that the identification

of the critical state is closely related to the early diagnosis of complex diseases.

Second, the saddle is the most important point on the boundary of two adjacent attraction basins. According to the Freidlin-Wentzell theory, when the system escapes from one attraction basin to another, it must cross the boundary around a specific point where the quasi-potential attains its minimum. To see this, we simulate the time course of the levels of proteins X and Y in an individual cell based on the stochastic system (1) (Figure 2B). The simulation result shows that the protein levels of the cell stay around the attractors at most times and cross the boundary of two attraction basins around the saddle, which is exactly the minimum point of the potential  $U(a, x, y)$  on the boundary.

Third, the saddle characterizes a critical state of the transition between multiple attraction basins. To accomplish stochastic phenotype switching, the system needs first to climb up the potential from one attractor to the saddle, and then to fall down the potential from the saddle to another attractor. Before reaching the saddle, the accumulation of stochastic forces will drive the system to climb up the potential against the potential gradient. This process in general will take rather a long time. Once the system crosses the saddle, it will reach another attractor along the potential gradient in a very short time. This shows that the dynamic features of a multistable system before and after reaching the saddle are totally different. To be more precise, let  $T_u$  denote the time needed for the system to climb up the potential and let  $T_d$  denote the time needed for the system to fall down the potential. The Freidlin-Wentzell theory shows that the ratio of  $T_u$  to  $T_d$  has the time scale of  $\exp(1/\varepsilon)$ . This suggests that the process of climbing up the potential is much longer than that of falling down the potential, which is consistent with the old saying: Diseases come on horseback, but go away on foot.

### Identification of the critical state

The critical state of a multistable system is important in many ways. Thus it is natural to ask whether we can identify the critical state in an effective way based on the noisy data of gene expression. Recently, Chen et al. [58] have developed a method of identifying the leading network in complex diseases by evaluating a kind of network entropy, and Gore et al. [59] have used generic statistical indicators to provide early warning signals for catastrophic collapse in the budding yeast population. Inspired by their ideas, in this section, we shall develop an effective method to identify the critical state of a multistable system using the time-course data of gene expression. Moreover, we shall validate the effectiveness of our method through both theoretical derivations and

numerical simulation.

We have seen that at certain ranges of the inducer concentration, the pivotal gene, gene  $X$ , has two steady-state expression levels,  $x_L$  and  $x_H$ , and a critical expression level  $x_M$ . We assume that we have measured the level of protein  $X$  in each individual cell within a bacterial population at two times,  $t$  and  $t + h$ , where the interval  $h$  of two successive measurements is chosen to have the time scale of  $1/\varepsilon$ , which is much shorter than the time scale  $\exp(1/\varepsilon)$  of stochastic phenotype switching. Intuitively, if the protein level in an individual cell is around  $x_L$  or  $x_H$  at time  $t$ , then the protein level at time  $t + h$  should be also around  $x_L$  or  $x_H$  since the interval  $h$  is much shorter than the time needed for stochastic phenotype switching (Figure 4A). However, if the protein level in an individual cell is around  $x_M$  at time  $t$ , then the protein level at time  $t + h$  will become rather scattered since the critical state is rather unstable (Figure 4A).

Let  $x(t)$  denote the level of protein  $X$  at time  $t$ , whose value can differ significantly between two individual cells. The above discussion illuminates us to define the variance  $D(x)$  at  $x$  as the variance of  $x(t + h)$  conditioned on the information of  $x(t) = x$ . More precisely, we define the variance  $D(x)$  at  $x$  as

$$D(x) = \text{Variance}(x(t + h)|x(t) = x), \quad (9)$$

where  $\text{Variance}(Z) = \langle (Z - \langle Z \rangle)^2 \rangle$  is the variance of the random variable  $Z$ . According to the above discussion, the variance  $D(x)$  around  $x_L$  or  $x_H$  should be small since the distribution of  $x(t + h)$  will be rather concentrated if  $x(t)$  is around  $x_L$  or  $x_H$ , whereas the variance  $D(x)$  around  $x_M$  should be large since the distribution of  $x(t + h)$  will be rather scattered if  $x(t)$  is around  $x_M$ . This suggests that we may detect the critical state by seeking the maximum point of the variance function  $D(x)$ .

We next validate the above intuitive discussion from the theoretical point of view. In fact, the theoretical expression of the variance function  $D(x)$  has the following form (see Supplementary Information):

$$D(x) \doteq (x_H - x_L)^2 p_L(x) p_H(x) + \varepsilon \left( \frac{p_L(x)}{\kappa_L} + \frac{p_H(x)}{\kappa_H} \right), \quad (10)$$

where  $p_L(x)$  and  $p_H(x)$  are two functions (see Supplementary Information for specific expressions) satisfying  $p_L(x) + p_H(x) = 1$ . We denote the maximum point of the variance function  $D(x)$  by  $x_{\max}$ . By Equation (10), we can easily see that  $x_{\max}$  satisfies

$$p_H(x_{\max}) = \frac{1}{2} + \frac{(\kappa_L - \kappa_H)\varepsilon}{2(x_H - x_L)^2 \kappa_L \kappa_H}. \quad (11)$$

In order to find the location of the maximum point  $x_{\max}$ ,

we depict the graph of the function  $p_H(x)$  in Figure 4B, from which we see that the function  $p_H(x)$  is sigmoidal with a critical transition around  $x_M$ . With the decrease of the noise level  $\varepsilon$ , the slope of the function  $p_H(x)$  at  $x_M$  tends to infinity. This fact, together with Equation (11), indicates that when the noise level  $\varepsilon$  is small, the maximum point  $x_{\max}$  of the variance function  $D(x)$  is very close to  $x_M$ . This suggests that the variance function  $D(x)$  may provide a clear signal for the position of the critical state.

A natural and important question is that whether we can estimate the variance function  $D(x)$  from the noisy data of gene expression. The answer is of course affirmative. Recent experimental techniques such as fluorescent labeling and microfluidic devices allow us to measure the expression level of the pivotal gene in each individual cell within a bacterial population at a series of times  $t_1, t_2, \dots, t_m$  with interval  $h$ . We assume that the experimental data of the  $n$ -th cell have the form of  $x(n, t_1), x(n, t_2), \dots, x(n, t_m)$ , where  $x(n, t_i)$  represents the expression level of the  $n$ -th cell at time  $t_i$ . For each time  $t_i$ , if  $x(n, t_i)$  is in a given small neighborhood of  $x$ , we pick out its next datum  $x(n, t_{i+1})$ , whereas if  $x(n, t_i)$  is not in the given small neighborhood of  $x$ , we throw away its next datum. By evaluating the sample variance of those data which are picked out, we can obtain a good estimation of the variance  $D(x)$  at  $x$ .

To validate the effectiveness of our method, we simulate the time course of the level of protein  $X$  in 4,800 virtual cells based on the stochastic model (1) and estimate the variance  $D(x)$  at several discrete levels of  $x$  (red circles in Figure 4C), from which we see that the simulation result coincides perfectly with the theoretical result (blue line in Figure 4C). Moreover, we see that the variance function  $D(x)$  changes drastically around  $x_M$ , whereas there is no significant change in  $D(x)$  around  $x_L$  and  $x_H$  (Figure 4C). This suggests that our method is effective in detecting the critical state of a multistable system using the noisy data of gene expression, even if no detailed mathematical model is available.

Before leaving this section, we would like to point out that our method of identifying the critical state is not only effective in simple multistable systems with stable fixed points, but also effective in complicated multistable systems with periodic orbits or stable limit cycles, in which case the time-course data of the system will oscillate. To see this, we consider the following two-dimensional system of SDEs:

$$\begin{cases} \dot{x} = y + \sqrt{2\varepsilon}\xi_x, \\ \dot{y} = -x^3 + x + \sqrt{2\eta}\xi_y, \end{cases} \quad (12)$$

where  $\varepsilon$  and  $\eta$  are two noise levels and  $\xi_x$  and  $\xi_y$  are two independent standard white noises. If  $\varepsilon = \eta = 0$ , then the

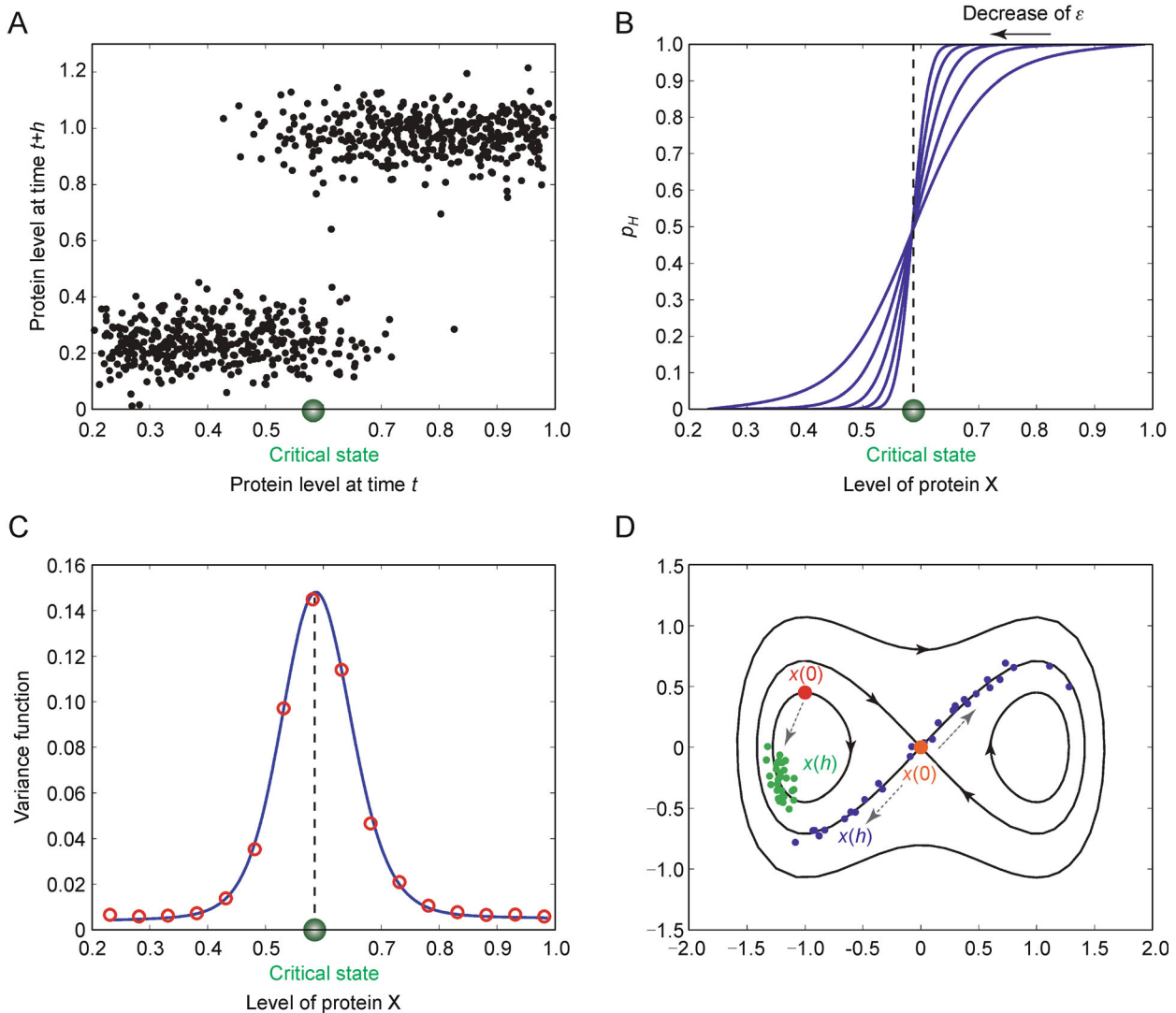


**Figure 4. Identification of the critical state.** (A) The simulation result of the level of protein X at two times,  $t$  and  $t + h$ , for an ensemble of 760 samples. The samples at time  $t + h$  are rather concentrated if the protein level is around  $x_L$  or  $x_H$  at time  $t$ , whereas those are rather scattered if the protein level is around  $x_M$  at time  $t$ . (B) The graph of the function  $p_H(x)$ . The function  $p_H(x)$  experiences a critical transition around the critical state  $x_M$ . With the decrease of the noise level  $\epsilon$ , the slope of the function  $p_H(x)$  at  $x_M$  tends to infinity. (C) The variance function  $D(x)$ . The variance  $D(x)$  at  $x$  is defined as the variance of the level of protein X at time  $t + h$  conditioned on the information that the protein level equals  $x$  at time  $t$ . The blue line represents the theoretical curve of the variance function and each red circle represents the simulation result based on the simulated dynamics of 300 virtual cells. The variance function changes slowly around the stable fixed points,  $x_L$  and  $x_H$ , and experiences a drastic change around the critical state  $x_M$ . (D) A multistable stochastic system with periodic orbits. The lines with arrows give the phase portrait the system. The origin  $(0, 0)$  (orange dot) is the unique critical point (saddle) of the system. The system has many periodic orbits inside and outside the two homoclinic orbits. We simulate the dynamics of the system at time  $h = 3.5$  for an ensemble of 60 samples under two different initial values (red and orange dots). The green dots represent the samples at time  $h$  when the system starts from the point  $(-1, 0.45)$  (red dot) on a periodic orbit and the blue dots represent the samples at time  $h$  when the system starts from the critical point (orange dot).

stochastic system is reduced to a deterministic system whose phase portrait is illustrated in Figure 4D. The origin  $(0, 0)$  (orange dot) is the only saddle and thus is the only critical point of the system. Interestingly, the stable

and unstable manifolds at the critical point match up exactly, forming two homoclinic orbits. Moreover, the system has many periodic orbits inside and outside the two homoclinic orbits.

To see whether our method can be applied to identify the critical point of the stochastic system (12), we simulate the dynamics of the system at time  $h = 3.5$  for an ensemble of 60 samples under two different initial values (red and orange dots) (Figure 4D). The simulation result shows that the samples at time  $h$  (green dots) are rather concentrated if the system starts from the point  $(-1, 0.45)$  (red dot) on a periodic orbit, whereas the samples at time  $h$  (blue dots) become rather scattered if the system starts from the critical point (orange dot). This suggests that the variance at the critical point is much larger than the variances at the points lying on the periodic orbits. Accordingly, we see that our method of identifying the critical state by seeking the maximum point of the variance function may be applied to various complicated multistable systems, not restricted to simple multistable systems with stable fixed points, such as the stochastic system (1).

## DISCUSSION

### Comparison with the previous work

Multistability in biologic systems has been widely studied in recent two decades and it has become an important recurring theme in cell signaling. In this paper, we study a class of multistable biologic systems, i.e., heterogeneous bacterial populations with stochastic phenotype switching and also provide a data-driven method to identify the critical state of multistable bacterial systems. In recent literature, an influential paper about multistability is the paper of Angeli et al. [60], who studied a large class of biologic systems with positive feedbacks and also provided a method of detecting bistability, bifurcations, and hysteresis in these systems. The themes of their paper is closely related to ours. Thus we find it necessary to discuss the similarities and differences between their paper and ours.

First, both the paper of Angeli et al. [60] and ours studied multistability in biologic systems with a positive-feedback network. Recent studies show that multistability always arises in biologic systems that contain a positive-feedback loop and it has been proved that the existence of at least one positive-feedback loop is a necessary condition for the existence of multiple steady states [61–63]. In our paper, we show that phenotypic heterogeneity in bacterial populations often results from the underlying double-positive-feedback gene networks, which is consistent with the above theoretical results.

Second, the paper of Angeli et al. [60] studied the deterministic nonlinear dynamics of multistable biologic systems and our paper studies the stochastic nonlinear dynamics of heterogeneous bacterial populations. In fact, deterministic models may lead to phenotypic heteroge-

neity, but they cannot explain the widely observed phenomena of stochastic phenotype switching and bet-hedging. In our paper, we use our stochastic model to provide a clear description of stochastic phenotype switching and bet-hedging within heterogeneous bacterial populations and study the role that stochastic effects play in generating these important experimental phenomena.

Third, in the paper of Angeli et al. [60], the relationship between the deterministic model of multistable systems and the widely used Markov chain model of population evolution is not clear. In our paper, we use the Freidlin-Wentzell theory to show that our stochastic model at the molecular level can be approximated by a Markov chain model at the cellular level, which reflects the long-term dynamics of multistable bacterial systems, when the noise level is small. It turns out that only by considering the stochastic dynamics of multistable bacterial systems can we unify the models at the two different levels.

Fourth, the paper of Angeli et al. [60] provided a possible method to detect multistability and bifurcations in a class of multistable systems satisfying the so-called “monotonicity” and “open-loop steady-state response” assumptions. Their method strongly depends on the properties of the system when the feedback is blocked. To detect multistability and bifurcations, the response data of the open-loop, feedback-blocked system to input stimuli must be obtained. This requirement is obvious too strong for realistic biologic systems. In our paper, however, we provide an effective data-driven method to identify the critical state of multistable biologic systems. In our method, only the time-course data of gene expression in individual cells are needed, even if no detailed mathematical model is available.

### Rationality of our stochastic model

In our stochastic model, we have used white noises with two different noise levels to describe the stochastic fluctuations in proteins X and Y, respectively. In this subsection, we shall explain the rationality of this assumption. The content of this section is somewhat technical. Readers who are unfamiliar with the knowledge of stochastic processes can skip this part.

In fact, the most precise model of the gene network in living cells is the chemical master equation (CME) [64]. Mathematically, the CME is the equation satisfied by the probability distribution of a Markov jump process which describes the copy number fluctuations of all participating macromolecules in the gene network. However, the dimension of the CME model is often so high that the theoretical expressions of many important quantities related to the system cannot be explicitly calculated. This makes the CME model difficult to be directly applied to practical problems with experimental data and

observations.

To simplify the CME model, Kurtz [65–67] proved in his pioneering work that every CME model can be approximated reasonably well by the so-called chemical Langevin equation when the volume of the system is large. Mathematically, the chemical Langevin Equation [68] is the equation satisfied by the probability distribution of an SDE model which describes the concentration fluctuations of all participating macromolecules in the gene network. To be more precise, we assume that there are  $n$  macromolecules involved in the gene network whose concentrations are denoted by  $x_1, x_2, \dots, x_n$ . The general form of an SDE model which governs  $x_1, x_2, \dots, x_n$  is given by

$$\dot{x} = b_i(x) + \sqrt{2\varepsilon_i} \sum_{j=1}^n \sigma_{ij}(x) \xi_j, \quad i = 1, 2, \dots, n, \quad (13)$$

where  $x = (x_1, x_2, \dots, x_n)$ ,  $b(x) = (b_1(x), b_2(x), \dots, b_n(x))$  is the drift coefficient of the SDE,  $\sigma(x) = (\sigma_{ij}(x))_{n \times n}$  is the diffusion coefficient of the SDE, and  $\xi_1, \xi_2, \dots, \xi_n$  are  $n$  independent standard white noises. Mathematically, it can be proved that when the matrix  $\sigma(x)$  is bounded from both below and above, almost all the major properties of the SDE model related to the Freidlin-Wentzell theory will change little if  $\sigma(x)$  is regarded as the identity matrix [54,57], in which case the SDE model (13) can be simplified as

$$\dot{x}_i = b_i(x) + \sqrt{2\varepsilon_i} \xi_i, \quad i = 1, 2, \dots, n, \quad (14)$$

In fact, the SDE has been applied to model the concentration fluctuations of macromolecules in gene networks in some previous studies [20]. Some reviews on this topic can be found in Refs. [69–71].

In the core double-positive-feedback gene network depicted in Figure 1E, there are only two participating macromolecules, proteins  $X$  and  $Y$ , if the inducer concentration is regarded as a parameter. In this case, the simplified SDE model (14) is exactly our two-dimensional stochastic model (1). To make biologists, especially experimental biologists, understand the main results of this paper, we would like to use white noises to describe stochasticity in gene expression and use the simplified SDE (14) to model multistable bacterial systems. Under this simplification, our stochastic model (1) can be simply understood as the random perturbation of the traditional deterministic model.

### Strengths and deficiencies of the SDE model

Just as George Box's famous saying goes, all models are wrong, but some are useful. Our model is no exception. In this paper, we use the SDE to model the concentration

fluctuations of the participating macromolecules in the gene network of heterogenous bacterial populations. However, the SDE model proposed in this paper has some deficiencies. In fact, in living bacterial systems, some macromolecules, such as mRNA and protein molecules, may exist at very low copy numbers [52], in which case the concept of concentration makes no sense. Thus the SDE model cannot provide a good approximation of the CME model when the copy numbers of the participating macromolecules are very small.

However, compared with the CME model, the SDE model proposed in this paper has many strengths. First, the dimension of the CME model is often too high to be directly applied to practical problems with experimental data and observations. If the gene network of the bacterial system contains  $n$  macromolecules and the maximal possible copy numbers of these  $n$  macromolecules are  $N_1, N_2, \dots, N_n$ . Then the dimension of the CME model will be  $N_1 N_2 \dots N_n$ . However, the SDE model compresses the dimension of the system to a large extent. If the gene network of the bacterial system contains  $n$  macromolecules, then the dimension of the SDE model is only  $n$ . This makes the system easy to be analyzed and makes many important quantities related to the system easy to be explicitly calculated.

Second, the mathematical theory of the SDE model is well developed, whereas that of the CME model is poorly developed due to its high complexity. In this paper, we use the Freidlin-Wentzell theory to explain stochastic phenotype switching and bet-hedging within isogenic bacterial populations and the consistence between our stochastic model and the traditional Markov chain models of population evolution. We believe that an analog of the Freidlin-Wentzell theory must exist in the CME model. However, such a theory for the CME model is not well developed up till now.

Third, the CME model is so abstract that it is not easy for biologists to understand and follow. In fact, without some deep mathematical knowledge, it is very difficult to understand the relationship between the CME model and the traditional deterministic model. However, the SDE model can be simply viewed as the random perturbation of the deterministic model. This makes the SDE model easy to be understood for both theoretical and experimental biologists.

Due to these reasons, we choose to use the SDE to model heterogenous bacterial populations, instead of the CME. We believe that the SDE, or equivalently, the chemical Langevin equation, which does not lose much information of the complicated CME, is a useful tool in the modeling of gene regulatory networks with inherent noises and in the analysis of the stochastic nonlinear dynamics of biologic systems.

## Potential of our stochastic model

Given the small size of a cell and the small copy numbers of participating macromolecules, cellular processes during gene expression are inherently stochastic. In this paper, we establish a unified nonlinear stochastic model of multistable bacterial systems at the molecular level based on a core double-positive-feedback gene network (Figure 1E) and provide a clear description of phenotypic heterogeneity, stochastic phenotype switching, and bet-hedging within isogenic bacterial populations. Although we have used the expression levels of two stress-related genes to establish our model, we point out here that the variables in our model are not necessarily the expression levels of the stress-related genes, but can include more comprehensive indicators measured by flow cytometry and other techniques, such as FSC (roughly proportional to cell size), SSC (roughly proportional to cell granularity and complexity), and the ATP concentration (positively correlated with total cell energy).

In our recent study about antibiotic resistance of *Escherichia coli* (unpublished work), we found that the one-dimensional expression data of the hydrolase gene only lead to a monomodal distribution, but the multi-dimensional expression data of a group of stress-related genes lead to an apparent multimodal distribution. This phenomenon is described in this paper. Our simulation result shows that although the expression data of a group of genes are distributed within multiple attraction basins, their marginal distribution may overlap to a large extent so that we may not be able to observe a multimodal distribution if we only focus on the expression data of a single gene. In our future work, we shall further apply the general framework discussed in this paper to the specific problem of antibiotic resistance of *Escherichia coli*.

Biologic systems with multistability are ubiquitous in nature. Some fundamental cellular processes, such as decision-making processes in cell cycle progression [72], cell fate determination [73–76], and apoptosis [77,78], display multistable features. In addition, multistability is also involved in disease progression, which can be divided into a normal state, a pre-disease state, and a disease state [55,56]. Although various multistable biologic systems have different feedback regulatory networks, the mathematical structures behind them are quite similar. We hope that the stochastic approach discussed in this paper can give enlightenment to the understanding of biologic systems with multistability and to the analysis of the related new phenomena and new questions.

## SUPPLEMENTARY MATERIALS

The supplementary materials can be found online with this article at DOI 10.1007/s40484-014-0035-5.

## ACKNOWLEDGMENTS

The authors gratefully acknowledge Prof. Michael S. Waterman at the University of Southern California and Prof. Michael Q. Zhang at Tsinghua University for stimulating discussions. This work is supported by NSFC (Nos. 11271029 and 11171024).

## COMPLIANCE WITH ETHICS GUIDELINES

The authors Chen Jia, Minping Qian, Yu Kang and Daquan Jiang declare that they have no conflict of interests.

This article does not contain any studies with human or animal subjects performed by any of the authors.

## REFERENCES

1. Kussell, E. and Leibler, S. (2005) Phenotypic diversity, population growth, and information in fluctuating environments. *Science*, 309, 2075–2078
2. Smits, W. K., Kuipers, O. P. and Veening, J. W. (2006) Phenotypic variation in bacteria: the role of feedback regulation. *Nat. Rev. Microbiol.*, 4, 259–271
3. Dubnau, D. and Losick, R. (2006) Bistability in bacteria. *Mol. Microbiol.*, 61, 564–572
4. Avery, S. V. (2006) Microbial cell individuality and the underlying sources of heterogeneity. *Nat. Rev. Microbiol.*, 4, 577–587
5. Dhar, N. and McKinney, J. D. (2007) Microbial phenotypic heterogeneity and antibiotic tolerance. *Curr. Opin. Microbiol.*, 10, 30–38
6. Lu, T., Shen, T., Bennett, M. R., Wolynes, P. G. and Hasty, J. (2007) Phenotypic variability of growing cellular populations. *Proc. Natl. Acad. Sci. USA*, 104, 18982–18987
7. Veening, J. W., Smits, W. K. and Kuipers, O. P. (2008) Bistability, epigenetics, and bet-hedging in bacteria. *Annu. Rev. Microbiol.*, 62, 193–210
8. Fraser, D. and Kaern, M. (2009) A chance at survival: gene expression noise and phenotypic diversification strategies. *Mol. Microbiol.*, 71, 1333–1340
9. Jablonka, E. and Raz, G. (2009) Transgenerational epigenetic inheritance: prevalence, mechanisms, and implications for the study of heredity and evolution. *Q. Rev. Biol.*, 84, 131–176
10. Snijder, B. and Pelkmans, L. (2011) Origins of regulated cell-to-cell variability. *Nat. Rev. Mol. Cell Biol.*, 12, 119–125
11. Mao, J., Blanchard, A. E. and Lu, T. (2014) Slow and steady wins the race: a bacterial exploitative competition strategy in fluctuating environments. *ACS Synth. Biol.* doi: 10.1021/sb4002008
12. Rulands, S., Jahn, D. and Frey, E. (2014) Specialization and bet hedging in heterogeneous populations. *Phys. Rev. Lett.*, 113, 108102
13. Acar, M., Mettetal, J. T. and van Oudenaarden, A. (2008) Stochastic switching as a survival strategy in fluctuating environments. *Nat. Genet.*, 40, 471–475
14. Salathé, M., van Cleve, J. and Feldman, M. W. (2009) Evolution of stochastic switching rates in asymmetric fitness landscapes. *Genetics*, 182, 1159–1164
15. Leisner, M., Stingl, K., Frey, E. and Maier, B. (2008) Stochastic switching to competence. *Curr. Opin. Microbiol.*, 11, 553–559
16. Gaál, B., Pitchford, J. W. and Wood, A. J. (2010) Exact results for the evolution of stochastic switching in variable asymmetric environments. *Genetics*, 184, 1113–1119
17. Libby, E., Rainey, P. B. (2011) Exclusion rules, bottlenecks and the

- evolution of stochastic phenotype switching. *P. Roy. Soc. B-Biol. Sci.*, 278, 3574–3583
18. Rainey, P. B., Beaumont, H. J., Ferguson, G. C., Gallie, J., Kost, C., Libby, E. and Zhang, X. X. (2011) The evolutionary emergence of stochastic phenotype switching in bacteria. *Microb. Cell Fact.*, 10, Suppl, 1, S14
  19. Ozbudak, E. M., Thattai, M., Lim, H. N., Shraiman, B. I. and van Oudenaarden, A. (2004) Multistability in the lactose utilization network of *Escherichia coli*. *Nature*, 427, 737–740
  20. Süel, G. M., Garcia-Ojalvo, J., Liberman, L. M. and Elowitz, M. B. (2006) An excitable gene regulatory circuit induces transient cellular differentiation. *Nature*, 440, 545–550
  21. Tsang, J. and van Oudenaarden, A. (2006) Exciting fluctuations: monitoring competence induction dynamics at the single-cell level. *Mol. Syst. Biol.*, 2, 0025
  22. Schultz, D., Ben Jacob, E., Onuchic, J. N. and Wolynes, P. G. (2007) Molecular level stochastic model for competence cycles in *Bacillus subtilis*. *Proc. Natl. Acad. Sci. USA*, 104, 17582–17587
  23. Sonenshein, A.L., Hoch, J.A. and Losick R. (2002) *Bacillus subtilis* and its closest relatives: from genes to cells. Washington: American Society for Microbiology.
  24. Errington, J. (2003) Regulation of endospore formation in *Bacillus subtilis*. *Nat. Rev. Microbiol.*, 1, 117–126
  25. Morohashi, M., Ohashi, Y., Tani, S., Ishii, K., Itaya, M., Nanamiya, H., Kawamura, F., Tomita, M. and Soga, T. (2007) Model-based definition of population heterogeneity and its effects on metabolism in sporulating *Bacillus subtilis*. *J. Biochem.*, 142, 183–191
  26. de Jong, I. G., Veening, J. W. and Kuipers, O. P. (2010) Heterochronic phosphorelay gene expression as a source of heterogeneity in *Bacillus subtilis* spore formation. *J. Bacteriol.*, 192, 2053–2067
  27. Sureka K., Ghosh, B., Dasugpta, A., Basu J., Kundu, M. and Bose Z., (2008) Positive feedback and noise activate the stringent response regulator in mycobacteria. *PLoS One* 3, e1771.
  28. Gefen, O. and Balaban, N. Q. (2009) The importance of being persistent: heterogeneity of bacterial populations under antibiotic stress. *FEMS Microbiol. Rev.*, 33, 704–717
  29. Ghosh, S., Sureka, K., Ghosh, B., Bose, I., Basu, J. and Kundu, M. (2011) Phenotypic heterogeneity in mycobacterial stringent response. *BMC Syst. Biol.*, 5, 18
  30. Veening, J. W., Stewart, E. J., Berngruber, T. W., Taddei, F., Kuipers, O. P. and Hamoen, L. W. (2008) Bet-hedging and epigenetic inheritance in bacterial cell development. *Proc. Natl. Acad. Sci. USA*, 105, 4393–4398
  31. Beaumont, H. J., Gallie, J., Kost, C., Ferguson, G. C. and Rainey, P. B. (2009) Experimental evolution of bet hedging. *Nature*, 462, 90–93
  32. Wolf, D. M., Vazirani, V. V. and Arkin, A. P. (2005) Diversity in times of adversity: probabilistic strategies in microbial survival games. *J. Theor. Biol.*, 234, 227–253
  33. Gupta, P. B., Fillmore, C. M., Jiang, G., Shapira, S. D., Tao, K., Kuperwasser, C. and Lander, E. S. (2011) Stochastic state transitions give rise to phenotypic equilibrium in populations of cancer cells. *Cell*, 146, 633–644
  34. Zhou, D., Wu, D., Li, Z., Qian, M., and Zhang, M. Q. (2013) Population dynamics of cancer cells with cell state conversions. *Quant. Biol.*, 1, 1–8.
  35. Karmakar, R. and Bose, I. (2007) Positive feedback, stochasticity and genetic competence. *Phys. Biol.*, 4, 29–37
  36. Mitrophanov, A. Y. and Groisman, E. A. (2008) Positive feedback in cellular control systems. *BioEssays*, 30, 542–555
  37. Mantzaris, N. V. (2007) From single-cell genetic architecture to cell population dynamics: quantitatively decomposing the effects of different population heterogeneity sources for a genetic network with positive feedback architecture. *Biophys. J.*, 92, 4271–4288
  38. Vellela, M. and Qian, H. (2009) Stochastic dynamics and non-equilibrium thermodynamics of a bistable chemical system: the Schlögl model revisited. *J. R. Soc. Interface*, 6, 925–940
  39. Qian, H. and Bishop, L. M. (2010) The chemical master equation approach to nonequilibrium steady-state of open biochemical systems: linear single-molecule enzyme kinetics and nonlinear biochemical reaction networks. *Int. J. Mol. Sci.*, 11, 3472–3500
  40. Qian, H. (2011) Nonlinear stochastic dynamics of mesoscopic homogeneous biochemical reaction systems—an analytical theory. *Nonlinearity*, 24, R19–R49
  41. Ge, H. and Qian, H. (2011) Non-equilibrium phase transition in mesoscopic biochemical systems: from stochastic to nonlinear dynamics and beyond. *J. R. Soc. Interface*, 8, 107–116
  42. Qian, H. (2012) Cooperativity in cellular biochemical processes: noise-enhanced sensitivity, fluctuating enzyme, bistability with nonlinear feedback, and other mechanisms for sigmoidal responses. *Annu. Rev. Biophys.*, 41, 179–204
  43. Qian, H. and Ge, H. (2012) Mesoscopic biochemical basis of isogenetic inheritance and canalization: stochasticity, nonlinearity, and emergent landscape. *Mol Cell Biomech.*, 9, 1–30
  44. McAdams, H. H. and Arkin, A. (1997) Stochastic mechanisms in gene expression. *Proc. Natl. Acad. Sci. USA*, 94, 814–819
  45. Elowitz, M. B., Levine, A. J., Siggia, E. D. and Swain, P. S. (2002) Stochastic gene expression in a single cell. *Science*, 297, 1183–1186
  46. Ozbudak, E. M., Thattai, M., Kurtser, I., Grossman, A. D. and van Oudenaarden, A. (2002) Regulation of noise in the expression of a single gene. *Nat. Genet.*, 31, 69–73
  47. Paulsson, J. (2004) Summing up the noise in gene networks. *Nature*, 427, 415–418
  48. Kaern, M., Elston, T. C., Blake, W. J. and Collins, J. J. (2005) Stochasticity in gene expression: from theories to phenotypes. *Nat. Rev. Genet.*, 6, 451–464
  49. Raser, J. M. and O’Shea, E. K. (2005) Noise in gene expression: origins, consequences, and control. *Science*, 309, 2010–2013
  50. Cai, L., Friedman, N. and Xie, X. S. (2006) Stochastic protein expression in individual cells at the single molecule level. *Nature*, 440, 358–362
  51. Yu, J., Xiao, J., Ren, X., Lao, K. and Xie, X. S. (2006) Probing gene expression in live cells, one protein molecule at a time. *Science*, 311, 1600–1603
  52. Xie, X. S., Choi, P. J., Li, G. W., Lee, N. K. and Lia, G. (2008) Single-molecule approach to molecular biology in living bacterial cells. *Annu. Rev. Biophys.*, 37, 417–444
  53. Sanchez, A., Choubey, S. and Kondev, J. (2013) Regulation of noise in gene expression. *Annu. Rev. Biophys.*, 42, 469–491
  54. Freidlin, M. I., Szücs, J. and Wentzell, A. D. (2012) Random perturbations of dynamical systems, 3rd ed. New York: Springer-Verlag
  55. Kim, D., Rath, O., Kolch, W. and Cho, K. H. (2007) A hidden oncogenic positive feedback loop caused by crosstalk between Wnt and ERK pathways. *Oncogene*, 26, 4571–4579
  56. Kellershohn, N. and Laurent, M. (2001) Prion diseases: dynamics of the infection and properties of the bistable transition. *Biophys. J.*, 81, 2517–2529

57. Olivieri, E. and Vares, M. E. (2005) Large deviations and metastability. UK: Cambridge University Press.
58. Liu, R., Li, M.Y., Liu, Z.P., Wu, J.R., Chen, L.N. and Aihara, K. (2012) Identifying critical transitions and their leading biomolecular networks in complex diseases. *Sci. Rep.*, 2, 813
59. Dai, L., Vorselen, D., Korolev, K. S. and Gore, J. (2012) Generic indicators for loss of resilience before a tipping point leading to population collapse. *Science*, 336, 1175–1177
60. Angeli, D., Ferrell, J. E. Jr. and Sontag, E. D. (2004) Detection of multistability, bifurcations, and hysteresis in a large class of biological positive-feedback systems. *Proc. Natl. Acad. Sci. USA*, 101, 1822–1827
61. Gouzé, J. L. (1998) Positive and negative circuits in dynamical systems. *J. Biol. Syst.*, 6, 11–15
62. Snoussi, E. H. (1998) Necessary conditions for multistationarity and stable periodicity. *J. Biol. Syst.*, 6, 3–9
63. Cinquin, O. and Demongeot, J. (2002) Positive and negative feedback: striking a balance between necessary antagonists. *J. Theor. Biol.*, 216, 229–241
64. Gillespie, D. T. (1992) A rigorous derivation of the chemical master equation. *Physica A*, 188, 404–425
65. Kurtz, T. G. (1970) Solutions of ordinary differential equations as limits of pure jump Markov processes. *J. Appl. Probab.*, 7, 49–58
66. Kurtz, T. G. (1971) Limit theorems for sequences of jump Markov processes approximating ordinary differential processes. *J. Appl. Probab.*, 8, 344–356
67. Kurtz, T. G. (1972) The relationship between stochastic and deterministic models for chemical reactions. *J. Chem. Phys.*, 57, 2976–2978
68. Gillespie, D. T. (2000) The chemical Langevin equation. *J. Chem. Phys.*, 113, 297–306
69. Rao, C. V., Wolf, D. M. and Arkin, A. P. (2002) Control, exploitation and tolerance of intracellular noise. *Nature*, 420, 231–237
70. Wilkinson, D. J. (2009) Stochastic modelling for quantitative description of heterogeneous biological systems. *Nat. Rev. Genet.*, 10, 122–133
71. Meister, A., Du, C., Li, Y. H., Wong, W. H. (2014) Modeling stochastic noise in gene regulatory systems. *Quant. Biol.*, 2, 1–29
72. Yao, G., Lee, T. J., Mori, S., Nevins, J. R. and You, L. (2008) A bistable Rb-E2F switch underlies the restriction point. *Nat. Cell Biol.*, 10, 476–482
73. Ferrell, J. E. Jr and Machleder, E. M. (1998) The biochemical basis of an all-or-none cell fate switch in *Xenopus oocytes*. *Science*, 280, 895–898
74. Xiong, W. and Ferrell, J. E. Jr. (2003) A positive-feedback-based bistable ‘memory module’ that governs a cell fate decision. *Nature*, 426, 460–465
75. Corson, F. and Siggia, E. D. (2012) Geometry, epistasis, and developmental patterning. *Proc. Natl. Acad. Sci. USA*, 109, 5568–5575
76. Yan, L., Yang, M., Guo, H., Yang, L., Wu, J., Li, R., Liu, P., Lian, Y., Zheng, X., Yan, J., et al. (2013) Single-cell RNA-Seq profiling of human preimplantation embryos and embryonic stem cells. *Nat. Struct. Mol. Biol.*, 20, 1131–1139
77. Eissing, T., Conzelmann, H., Gilles, E. D., Allgöwer, F., Bullinger, E. and Scheurich, P. (2004) Bistability analyses of a caspase activation model for receptor-induced apoptosis. *J. Biol. Chem.*, 279, 36892–36897
78. Spencer, S. L., Gaudet, S., Albeck, J. G., Burke, J. M. and Sorger, P. K. (2009) Non-genetic origins of cell-to-cell variability in TRAIL-induced apoptosis. *Nature*, 459, 428–432